Kinetics of Soot Oxidation by NO_2

Manish Shirvastava[1], Anh Nguyen[(2,3)], Zhongqing Zheng[(2,3)], Hao-Wei Wu[(2,3)], and Heejung Jung[(2,3)]

1) Pacific Northwest National Laboratory, Richland, Washington
2) University of California, Riverside, Department of Mechanical Engineering
3) College of Engineering – Center for Environmental Research and Technology (CE-CERT)

As regulations for diesel particulate emissions have become stringent, diesel particulate filter (DPF) is recognized as one of the crucial after-treatment system in diesel vehicles. Hence, an improved understanding of the kinetics of diesel particle oxidation is necessary to optimally design the DPF. However, there are limitations to current kinetic data since they are mostly obtained under oxygen environment. Although new technologies convert NO to NO_2 upstream of the DPF to enhance soot oxidation at low exhaust temperatures, very few prior studies have considered NO_2 as a major oxidant. Also, kinetics of soot oxidation has been studied only using bulk methods such as thermogravimetric analysis (TGA), which leads to difficulties in separating reaction effects from heat and mass transfer effects.

This present work uses the online aerosol technique of high-temperature oxidation tandem differential mobility analysis (HTO-TDMA) to study kinetics of soot oxidation by NO_2 as shown in figure 1. In the experiment the polydisperse soot particles are generated by a diffusion flame burner using ethylene as fuel. Soot particles are sent to differential mobility analyzer DMA-1 (TSI 3081 series long column DMA) for size selection based on electrical mobility. Size-selected monodisperse soot particles from the first DMA are then oxidized in a high temperature flow reactor and the resulting particle size distribution is measured using the second DMA with a condensation particle counter (CPC) as the detector. Different mixing ratios of the oxidant NO_2 are introduced into the sheath flow of DMA-1 with N_2 as the carrier gas. N_2 (purity 99.999% Praxair) is mixed with base NO_2 gas (certified at 5049 ppm) in different proportions to get desired mixing ratio of NO_2 ranging 0-600 ppm. The furnace set-point temperatures were also varied in the range of 500-950 °C.

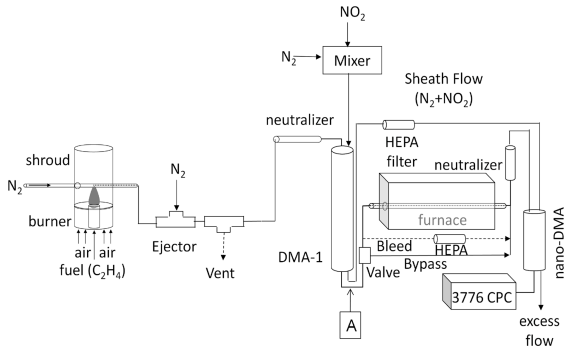

Figure 1 Schematic of experimental system

The temperature in furnace is measured with a K-type thermocouple for the furnace set-point temperatures. The axial temperature profile along the furnace is modeled by fitting a fourth-order polynomial fit to the experimental measurements as shown in figure 2. It can be seen that the temperature is maximum in the middle of the furnace and lowest at the inlet and exit. As can also be seen from the calculated NO_2 mixing ratios throughout the furnace, the ratios decrease at high temperature due to NO_2 decomposition. The graph also show the instantaneous soot oxidation rate (dDp/dt), which demonstrate that the rates vary along the furnace as a function of temperature and NO_2 mixing ratio.

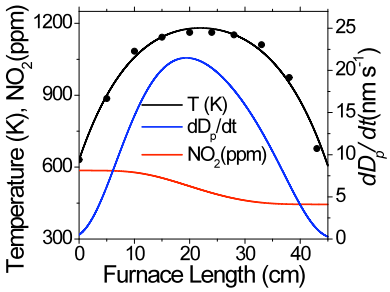

Figure 2 Variation of temperature, NO2 mixing ratio, and soot oxidation rate within the furnace at furnace set-point temperature of 850 °C and inlet NO2 mixing ratio of 600 ppm.

The results of TDMA scans from the nano-DMA for particles size of 40 nm show that particle shrinks due to both increasing temperatures and increasing oxidant levels. This is proven by figure 3. The figure shows that the particle

size distribution shifts to a lower size with increasing NO_2 mixing ratio at constant furnace set temperature as well as a reduction in sizes with constant NO_2 mixing ratio and increasing furnace temperatures. The broadening of particle size distribution with oxidation is because of particles experiencing a range of residence times within the reactor. The varying residence time distribution of particles is because of near-laminar gas flow, buoyancy-induced secondary flows at higher furnace temperatures, and effects of thermophoresis. During the experiment, it was interesting to find out that particles show modest size reduction even at zero NO_2 mixing ratios when nitrogen is the carrier gas at higher furnace temperatures. It is important to separate the non-oxidative size reduction from calculations of ΔDp to derive accurate oxidative kinetics of soot oxidation. Therefore, the oxidative component of the change in diameter is derived by subtracting the ΔDp measured under N_2 environment from the total ΔDp measured at any given NO_2 mixing ratio. In this work, the soot particles are found to have significant organic carbon content (OC) in addition to elemental carbon (EC). A thermal-optical analysis on the polydisperse soot particles collected on a quartz filter from the flame indicated that OC could be up to 40% of the total carbon (TC).

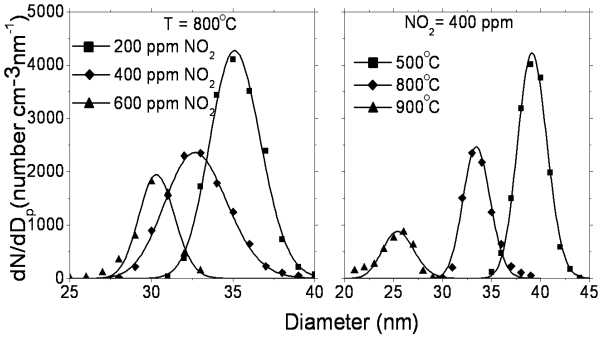

Figure 3 TDMA data showing particle number size distribution data (d*N*/d*D*p) for oxidation of 40 nm soot particles

The results from the analysis by assuming the reaction order as unity suggest that A_{soot} and E_{soot} values for oxidation to be 2.4×10-14 ($nmK^{0.5}s^{-1}$ cm^3 $molecule^1$) and 47.1 kJ mol^{-1}, respectively. This activation energy value is lower than those values reported by prior studies. A comparison is shown in Figure 4, illustrating the difference between the A_{soot} and E_{soot} values at different NO_2 mixing ratios with the soot oxidation rate in the presence of air (which has a high mixing ratio of 20% O_2) derived by previous study. The activation energy for soot oxidation with NO_2 is significantly lower than oxidation with air in the temperature range 800-900 °C. At lower temperatures (below 500°C), it is expected that oxidation with NO_2 to be greater than that with only O_2. Since parts per million levels of NO_2 cause soot oxidation at low temperatures, this suggest that NO_2 is a stronger oxidant than O_2. It is recommended to have future studies into understanding the kinetics of soot oxidation in the presence of other oxidants like O_2 and H_2O to improve soot emission control for both the in-cylinder and after-treatment system.

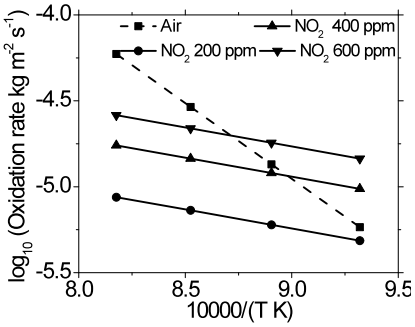

Figure 4 Comparison of soot oxidation rate at different NO_2 mixing ratios in the present study and soot oxidation rate in the presence of air derived by Higgins et al.

Kinetics of soot oxidation by NO_2

Manish Shrivastava, Anh Nguyen, Zhongqing Zheng, Hao-Wei Wu, and Heejung Jung

For questions and comments, please email: heejung@engr.ucr.edu

Motivation

Soot particles affect earth's climate and pose a significant human health risk. Soot emitted from vehicles could be controlled in 2 ways:

1. **Modifying combustion process inside the engine**
2. **Removing soot from exhaust stream**

Understanding kinetics of soot oxidation: Oxidants like O_2 and NO_2
NO_2 oxidation > O_2: Promoting low-temperature soot oxidation

Methods

Soot oxidation has been studied using offline methods such as thermo-gravimetric analysis (TGA) that are limited by:

1. **Heat and mass transfer diffusion limitations**
2. **Aging of collected soot on substrate**

Online aerosol technique: High temperature oxidation tandem differential mobility analysis (HTO-TDMA). In this study, the HTO-TDMA method was applied to study oxidation of near spherical 40 nm soot particles in the presence of NO_2.

Soot particles follow complex trajectories within the furnace due to:

- **Axially and radially varying temperature and velocity**
- **Recirculation**
- **Thermophoresis**

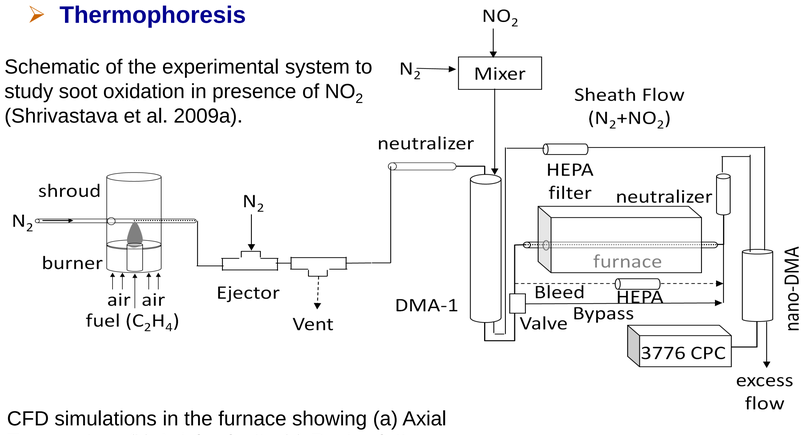

Schematic of the experimental system to study soot oxidation in presence of NO_2 (Shrivastava et al. 2009a).

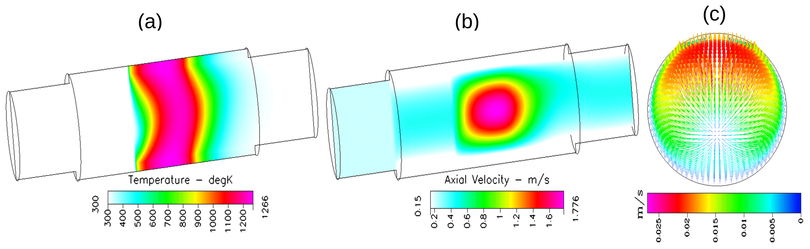

CFD simulations in the furnace showing (a) Axial Temperature (b) Axial velocity (c) Recirculating radial velocity patterns (Shrivastava et al. 2009b).

Kinetics

Oxidation rate of soot varies throughout the furnace due to variations in:

- **NO_2 concentrations**
- **Temperature**
- **Flow velocity**

At temperatures higher than 500 °C, NO_2 decomposed to NO within the furnace given by the well known reaction:

$$NO_2 + NO_2 \rightarrow O_2 + NO + NO \qquad \textbf{(1)}$$

The rate expression *k(T)* for Eq. (1) is defined as:

$$k(T) = A_{NO2}\exp(-\frac{E_{NO2}}{RT}) \qquad \textbf{(2)}$$

k(T): cm^{-3} $molecule^{-1}$ s^{-1}, A_{NO2} : Arrhenius rate constant, E_{NO2}: activation energy (kJ mol^{-1})

At any axial location within the furnace, the values of NO_2 concentration could be calculated as function of time and temperature using Eq. (2) and (3) given as:

$$\frac{1}{N_t} = k(T)t + \frac{1}{N_0} \qquad \textbf{(3)}$$

N_t : [NO_2](molecule cm^{-3}) at time *t* in seconds, N_0 : NO_2 concentration at furnace inlet (time zero)

The varying oxidation rate of particles was modeled using the following equation:

$$\dot{D}_p = -A_{soot}T^{1/2}\exp(-\frac{E_{soot}}{RT})(P_{NO2})^n \qquad \textbf{(4)}$$

A_{soot} nm $K^{-0.5}$ s^{-1} $(Nm^{-2})^{-n}$, E_{soot} kJ mol^{-1}
P_{NO2} :partial pressure of NO_2 in Nm^{-2},
n: reaction order of soot

The total decrease in particle size by oxidation in the furnace was found by integrating Eq. (4) along the furnace length:

$$\Delta D_p = \int_0^X \frac{\dot{D}_p(x)}{u(x)}dx \qquad \textbf{(5)}$$

Values of A_{soot} and E_{soot} in equation (4) were determined by fitting to measured values of ΔD_p.

Results

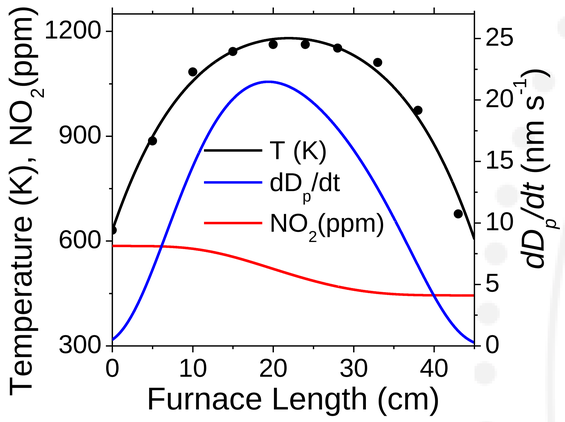

Variation of temperature, NO_2 concentrations, and soot oxidation rates in the furnace

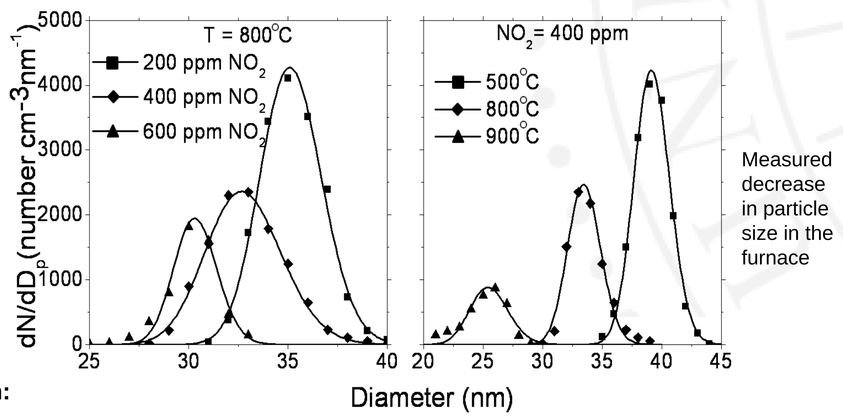

Measured decrease in particle size in the furnace

2 parameters A_{soot} and E_{soot} in Eq. (4) were fit to 15 measured ΔD_p values at:

- **3 different inlet NO_2 concentrations ranging 200-600 ppmv**
- **5 different furnace temperatures ranging 500-950 °C**

When reaction order *n* assumed to be unity, fitting results yielded:

- **E_{soot} : 47.1 kJ mol^{-1} using HTO-TDMA method**
- **Previous studies E_{soot} values ranged 60-76 kJ mol^{-1} using bulk methods**

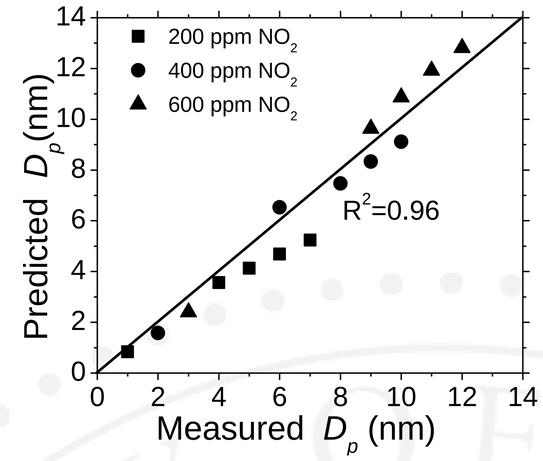

Quality of fits

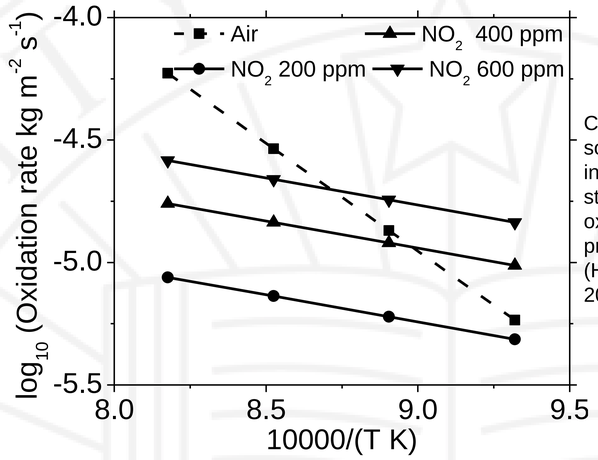

Comparison of soot oxidation rate in the present study vs. soot oxidation by air in previous study (Higgins et al. 2002).

Conclusions

- **HTO-TDMA method: Better mechanistic understanding of soot oxidation**
- **2 parameters fits: Represent a range of reaction conditions (Temperature and NO_2 concentrations)**
- **Implications: Semi-empirical modeling approach with a few parameters could describe soot oxidation both in-cylinder and at exhaust after-treatment conditions**
- **Future studies: Synergistic effects of NO_2 and O_2 on soot oxidation**

References

Higgins K.J., Jung H., Kittelson D.B., Roberts J.T., Zachariah M.R., *Size-selected nano-particle chemistry: kinetics of soot oxidation.* The Journal of Physical Chemistry A, 2002. **106**(1): p. 96-103.

Shrivastava M., Wu H.W., Nguyen A., Jung H., *Kinetics of soot oxidation by NO_2.* Aerosol Science and Technology, 2009a, **in preparation.**

Shrivastava M., Gidwani A., Jung H., *Modeling oxidation of soot particles within a laminar aerosol flow reactor using Computational Fluid Dynamics.* Aerosol Science and Technology, 2009b, **accepted for publication.**

Acknowledgements

This work was done at CE-CERT University of California, Riverside. A part of this research was also supported by the U.S. DOE's Atmospheric Systems Research Program under contract DE-AC06-76RCO 1830 at PNNL.

CE-CERT

UC RIVERSIDE UNIVERSITY OF CALIFORNIA

Pacific Northwest NATIONAL LABORATORY
Proudly Operated by Battelle Since 1965